Acoustic Field Around a Transonic Cavity Flow

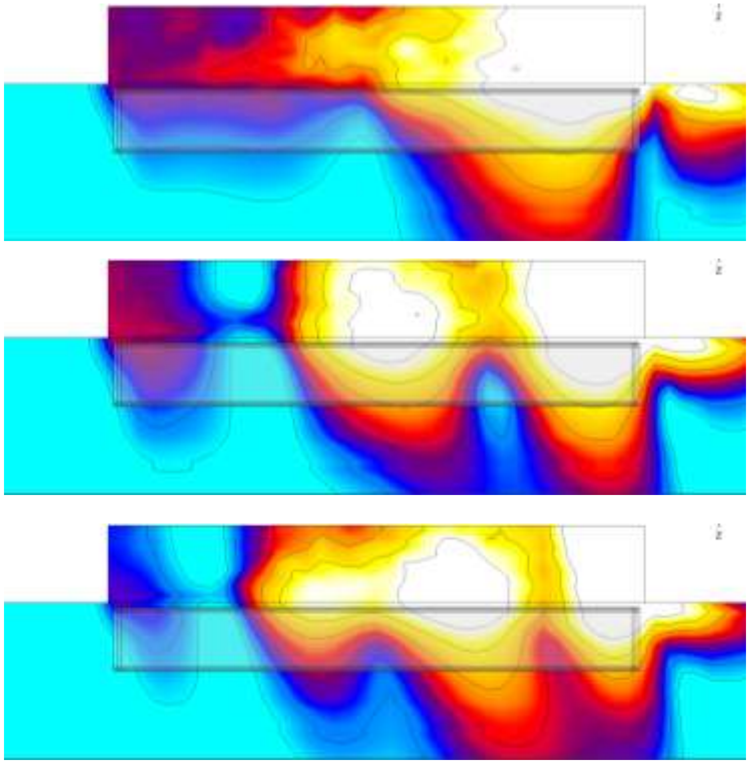

Gaëtan Loupy and George Barakos

CFD Laboratory
School of Engineering
University of Glasgow
James Watt South Building
G12 8QQ, Glasgow
George.barakos@glasgow.ac.uk

CEAA - Svetlogorsk (Russia) – 21/24 September 2016

Cavity Flow

- Weapon bay are used in modern aircraft:
  - UCAV.
  - F-35.

- Complex cavity flow physics:
  - **Feedback loop**.
  - Rossiter **modes**.
  - CFD needs LES, DES, SAS for this flow.

- Cavity flows are characterized by:
  - Large **unsteadiness**.
  - **High levels of noise**.
  - Complex waves/shear layer **interactions**.

- Leading to:
  - Structure **fatigue**.
  - **Stealth reduction**.
  - Store release **variability**.

Boeing X-45 Weapon Bay.

Schilieren image of a cavity flow at M=0.85.
DES simulation.

Noise Analysis

- Tools commonly used for cavity flows:
  - Sound Pressure Levels (SPL)
  - Overall Sound Pressure Levels (OASPL)

- Drawbacks:
  - Applicable in **wind tunnel** test to a **limited number of probe points**.
  - The **temporal fluctuations** are not know.

- Application of two more advanced noise field analysis:

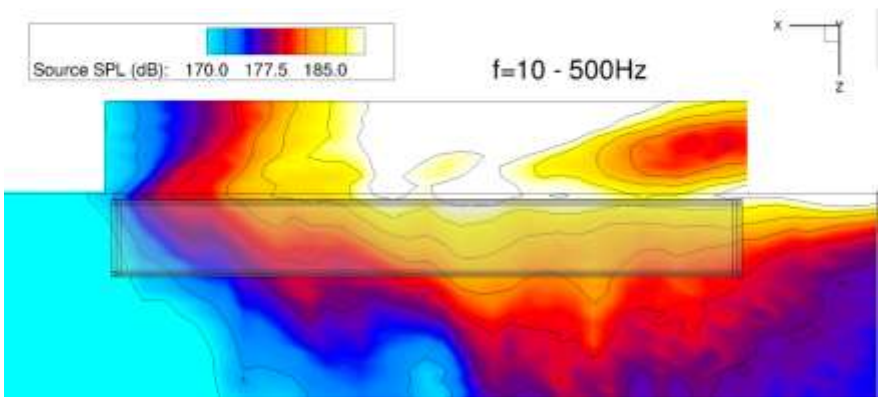

The **beamforming**: analysis of the **entire noise field** with a **microphone array**.

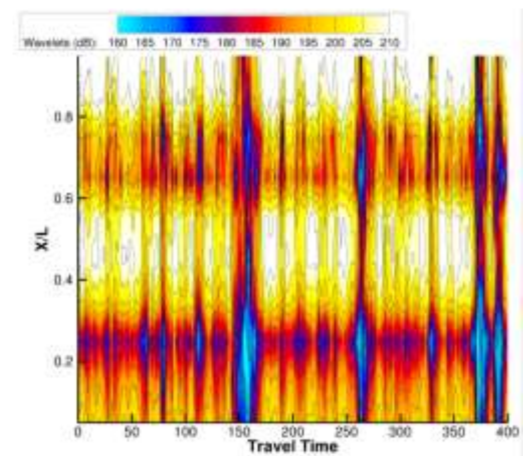

The **wavelet transform:** spatio-temporal analysis of the noise.

CFD Solver – Core HMB3 Features

- Control volume method
- **Parallel** - Shared and Distributed memory
- **Multi-block structured grids** - Complex geometries
- **Fully-Implicit** time marching / **Frequency** domain
- **Osher**, **Roe**, **AUSM+/UP** schemes for all Mach numbers
- **MUSCL** scheme for formally 3rd order accuracy
- Central differences for viscous fluxes
- Krylov subspace linear solver with pre-conditioning
- **RANS**, **URANS**, **LES**, **DES, SAS**, **turbulence** and **transition** models
- **Actuator Disk** method
- **Blade Actuation**, **Aeroelasticity** , **Rotor Trimming**
- **Moving/Deforming** grids, **Sliding Planes**, **Overset**
- **Steady Hover** formulation, **Unsteady Wind-tunnel** and **Vehicle** formulations
- **Adjoint Method** for computing aerodynamic derivatives
- **Validation Database**
- **Utilities** for processing data, structural models etc.
- **Used by Academics and Engineers**

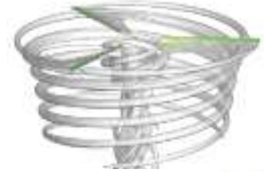
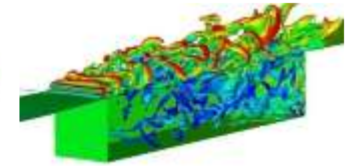
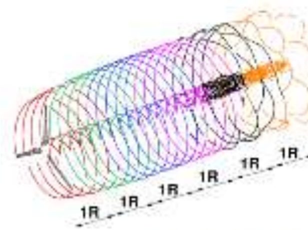
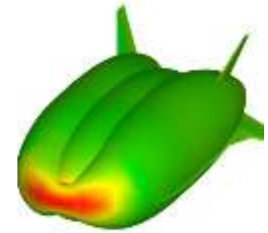
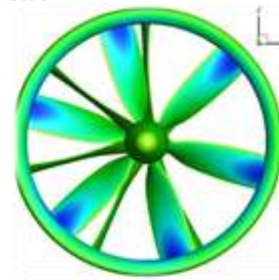


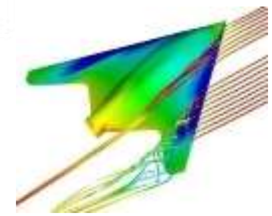

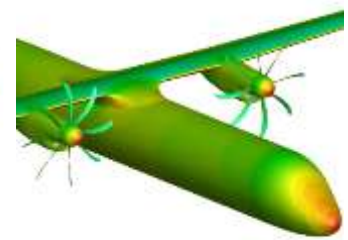

Cavity Computations with HMB

- Key journal papers:

  - Babu, S.V., Loupy, G.J.M., Dehaeze, F., Barakos, G.N., Taylor, N.J., ***Aeroelastic simulations*** *of stores in weapon bays using Detached-Eddy Simulation*, (2016) Journal of Fluids and Structures, 66, pp. 207-228.
  - Babu, S.V., Zografakis, G., Barakos, G.N., Evaluation of **scale-adaptive simulations** for transonic cavity flows, (2015) *Notes on Numerical Fluid Mechanics and Multidisciplinary Design*, 130, pp. 433-444.
  - Lawson, S.J., Barakos, G.N. Computational fluid dynamics analyses of **flow over weapons-bay geometries**, (2010) *Journal of Aircraft*, 47 (5), pp. 1605-1623.
  - Lawson, S.J., Barakos, G.N. Evaluation of des for weapons bays in **UCAV**s, (2010) *Aerospace Science and Technology*, 14 (6), pp. 397-414.
  - Nayyar, P., Barakos, G.N., Badcock, K.J. Numerical study of transonic cavity flows using **large-eddy** and **detached-eddy simulation** (2007) *Aeronautical Journal*, 111 (1117), pp. 153-164.
  - S.J. Lawson and G.N. Barakos. Review of Numerical Simulations For High-Speed, Turbulent Cavity Flows. *Progress in Aerospace Sciences*, 47(3):186 –216, 2011.
  - HMB is validated for cavity flows.

Geometry & Conditions

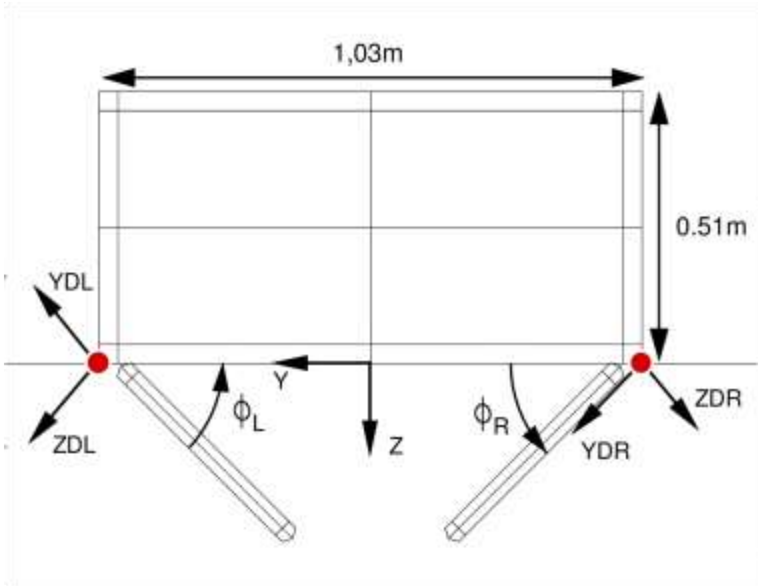

Downstream view of the axis systems

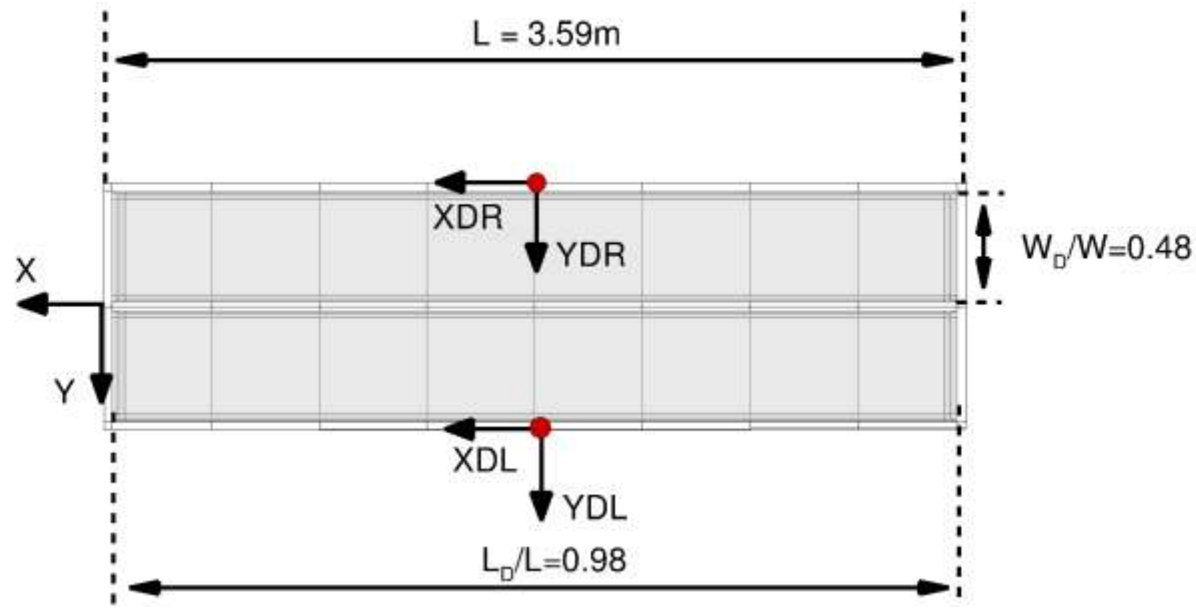

Bottom view of the axis systems

- Idealised clean cavity:
  - L=3,59m
  - L/D=7
  - W/D=2

- M=0.85
- Re_L=6.5million
- SAS k-ω
- dt=1% of bay crossing time
- 34 millions cells

Beamforming Analysis

- Use of a **microphone (sensor) array** for noise analysis:
  - Multi-spiral distribution.
  - 101 sensors.
  - 2 and 4 cavity depth from shear layer

- A grid of discrete points in space is scanned.

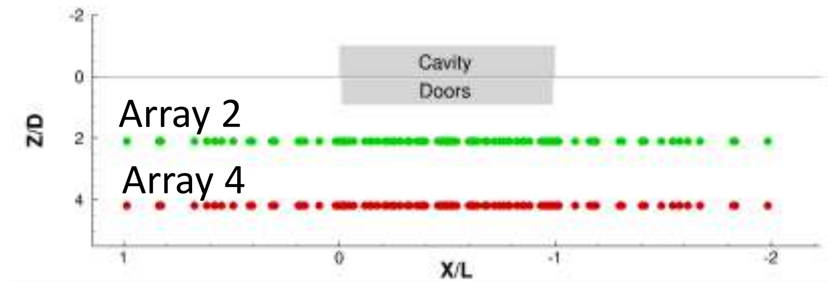

Side view of the microphone arrays

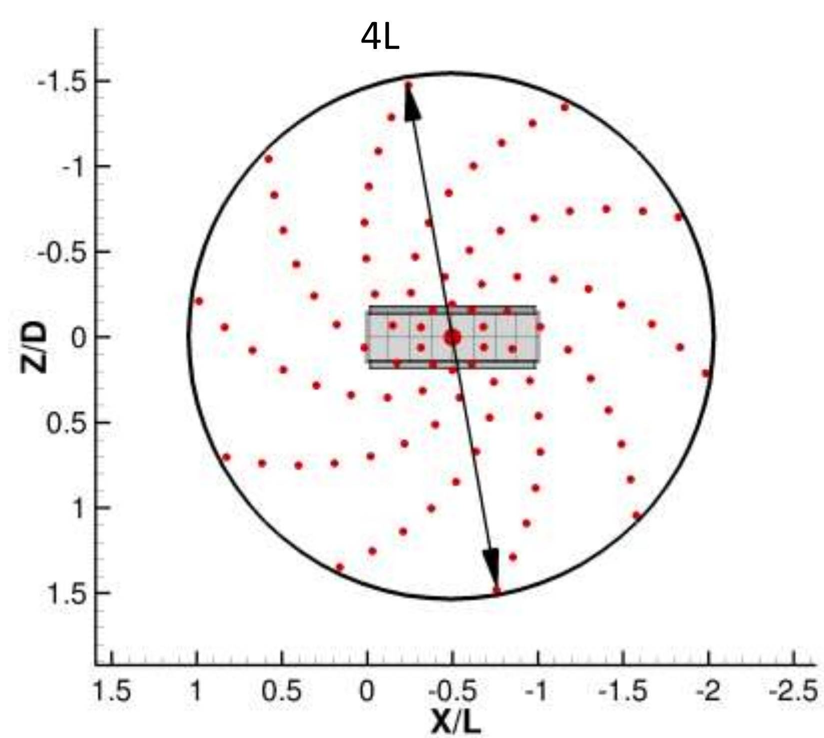

Top view of the microphone arrays

Beamforming Analysis

- Delay and Sum Beamforming:
  - For each of the *m* sensors a **time delay** Δ_m from the source and a reference sensor (0) is calculated:

$$\Delta_m \triangleq \frac{r_m - r_0}{c}$$

  - The beamformer output is given by $Z(\omega)$:

$$Z(\omega) = \mathcal{F}\left\{\sum_{m=0}^{M-1} y_m(t-\Delta_m)\right\} = \sum_{m=0}^{M-1} Y_\omega e^{-j\Delta_m \omega}.$$

$y_m(t)$ is the signal from each sensor.

  - The **accuracy** of the result depends on the **distances computation**:
    - Hypothesis on **wave propagation**.

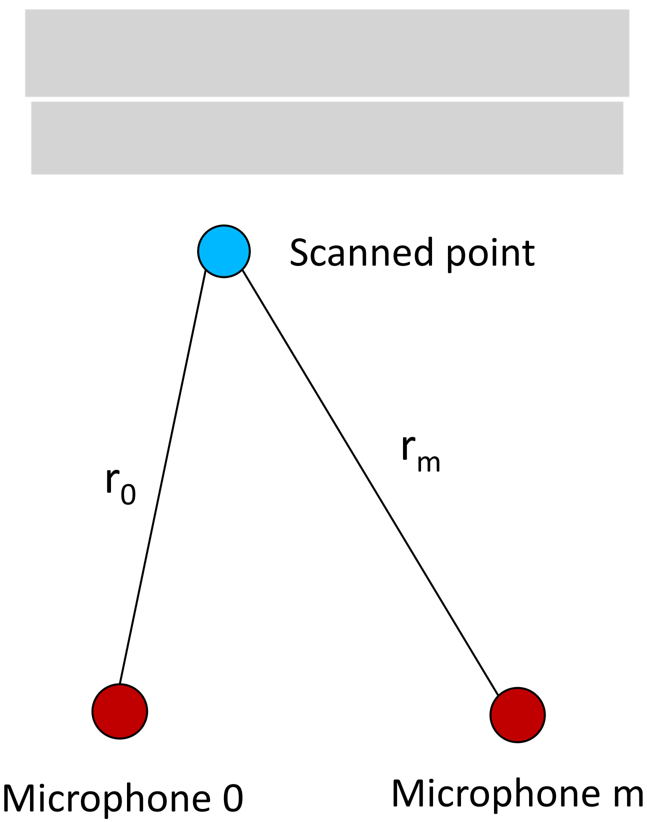

Distances computation with a planar waves propagation.

Computation of Distances

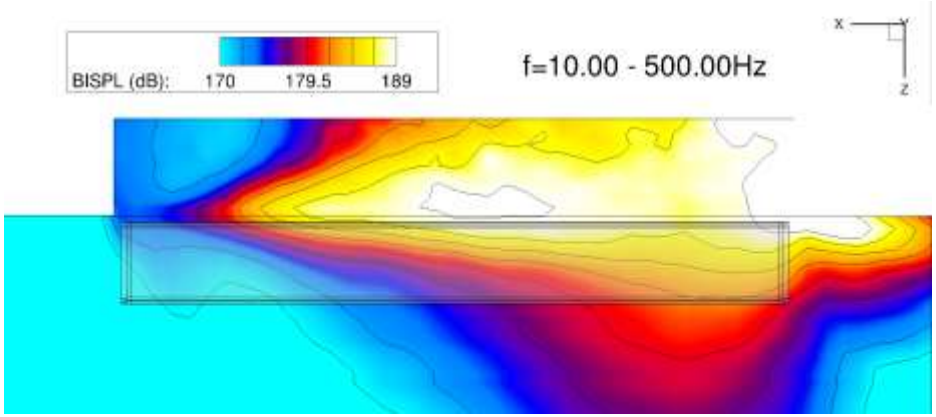

BISPL for fixed doors at 110 degrees.

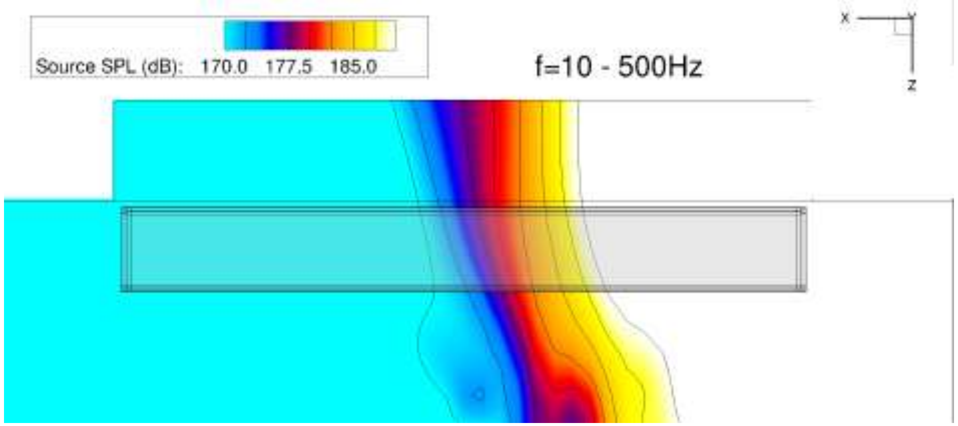

Beamforming for fixed doors at 110 degrees using the arrays 2 and 4.

- **Planar wave** propagation:
  - No matching with the BISPL.
  - This hypothesis is **not valid**.

- The velocity flowfield has to be taken into account:
  - Freestream at M0.85
  - The **waves are transported**.

Computation of Distances

1. The **path** from a **scan point to a microphone** is computed taking into account the **flowfield**.
2. The wave travel on a distance d_{travel} at a mean velocity c_{travel}.
3. The **equivalent distance** at a speed c is: $r_m = d_{travel} \dfrac{c}{c_{travel}}$

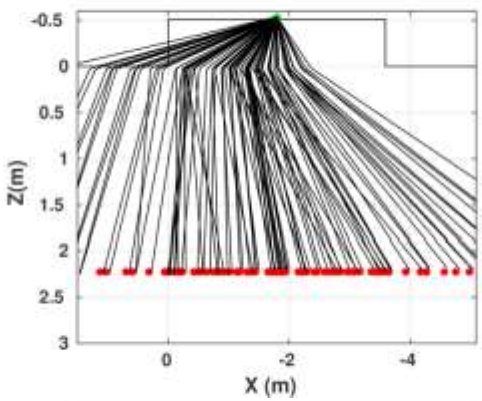

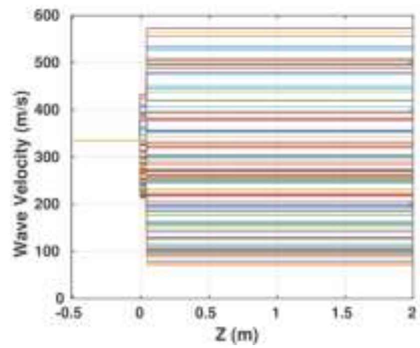

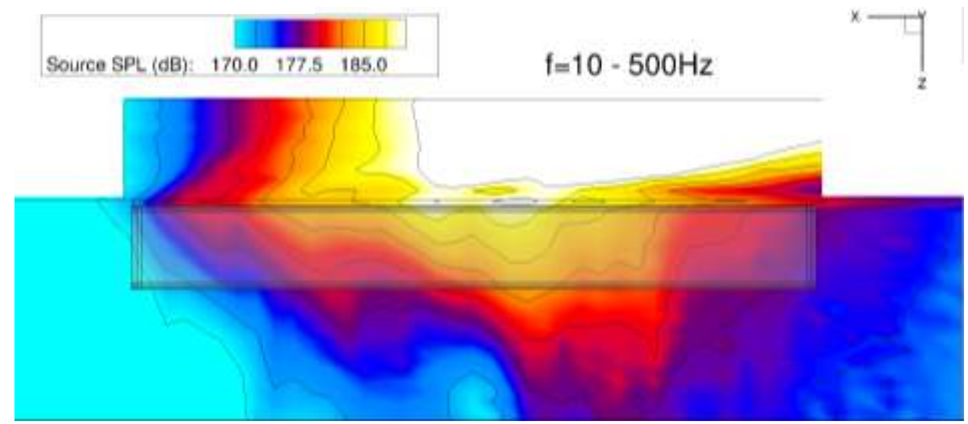

Ideal propagation model (Arrays 2 and 4).

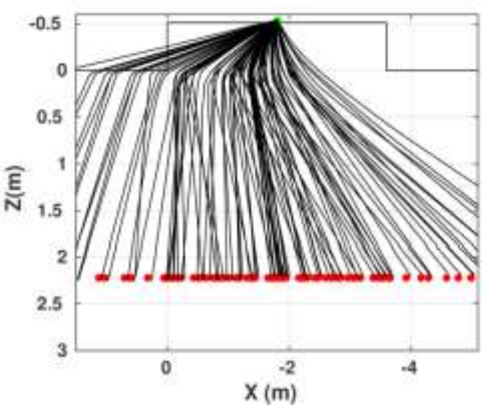

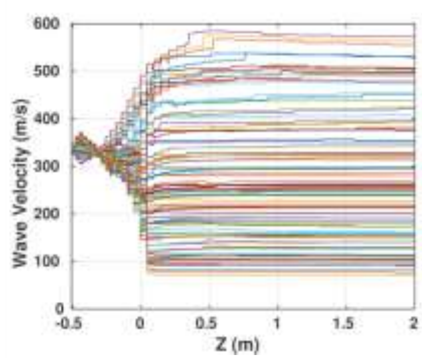

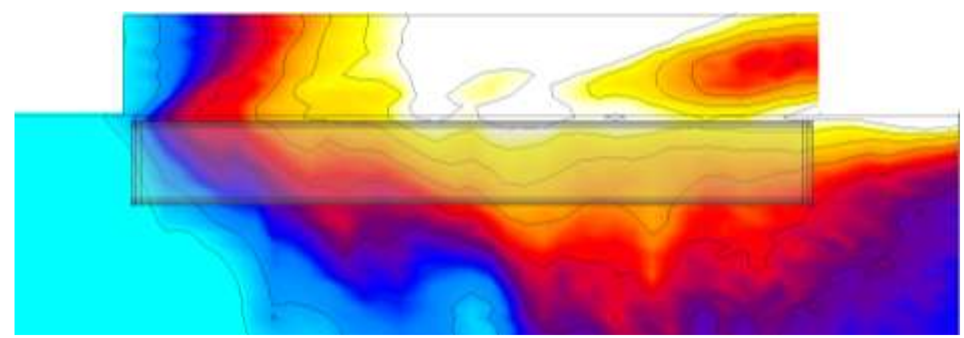

Full propagation model (Arrays 2 and 4).

Array Position

- Array 2 is **too close** to the cavity:
  - The shear layer is not captured.
- Array 4 has better result:
  - The shear layer is captured.
  - The middle source is not correctly localised.
- Arrays 2 and 4:
  - The two shear layer sources agree with the BISPL.
  - The **combination** give a **better vertical accuracy**.

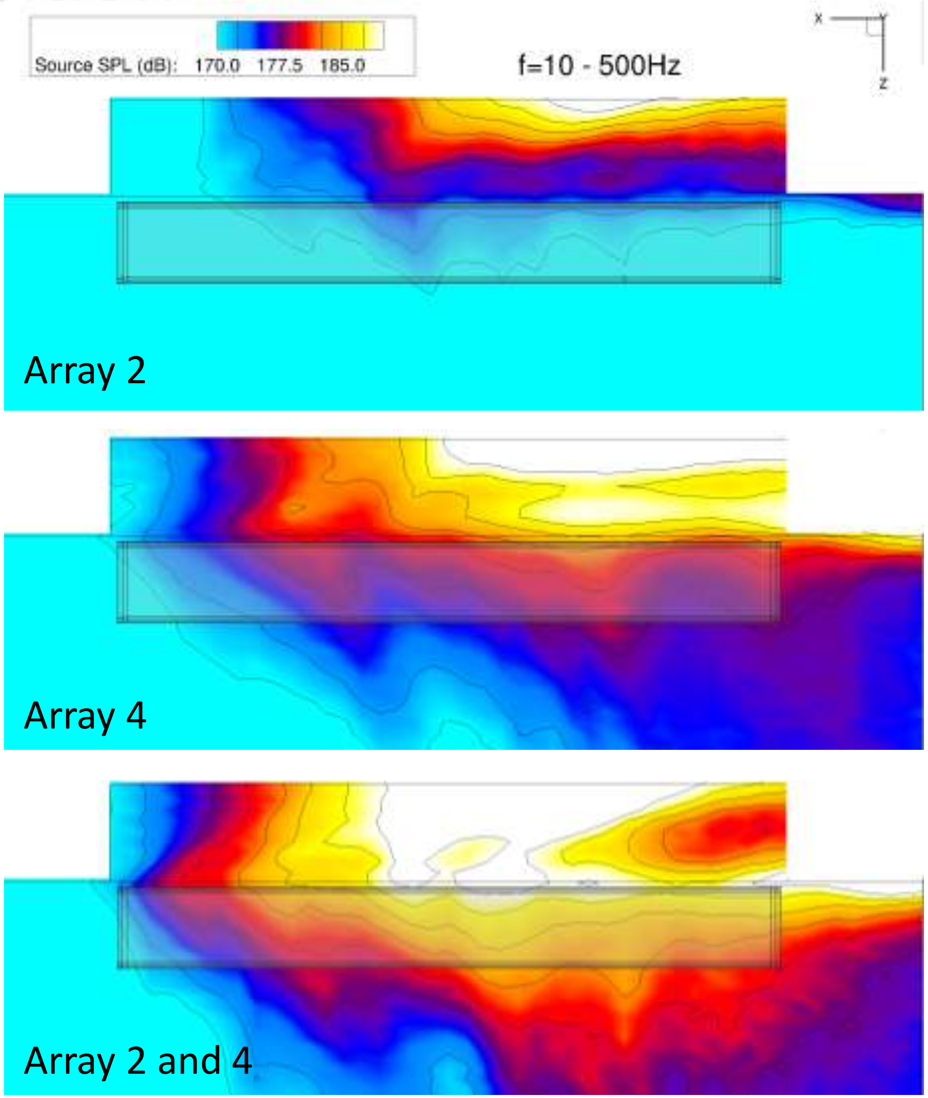

Beamforming for different array position with full propagation model. (Doors 110 degrees)

Mode shapes

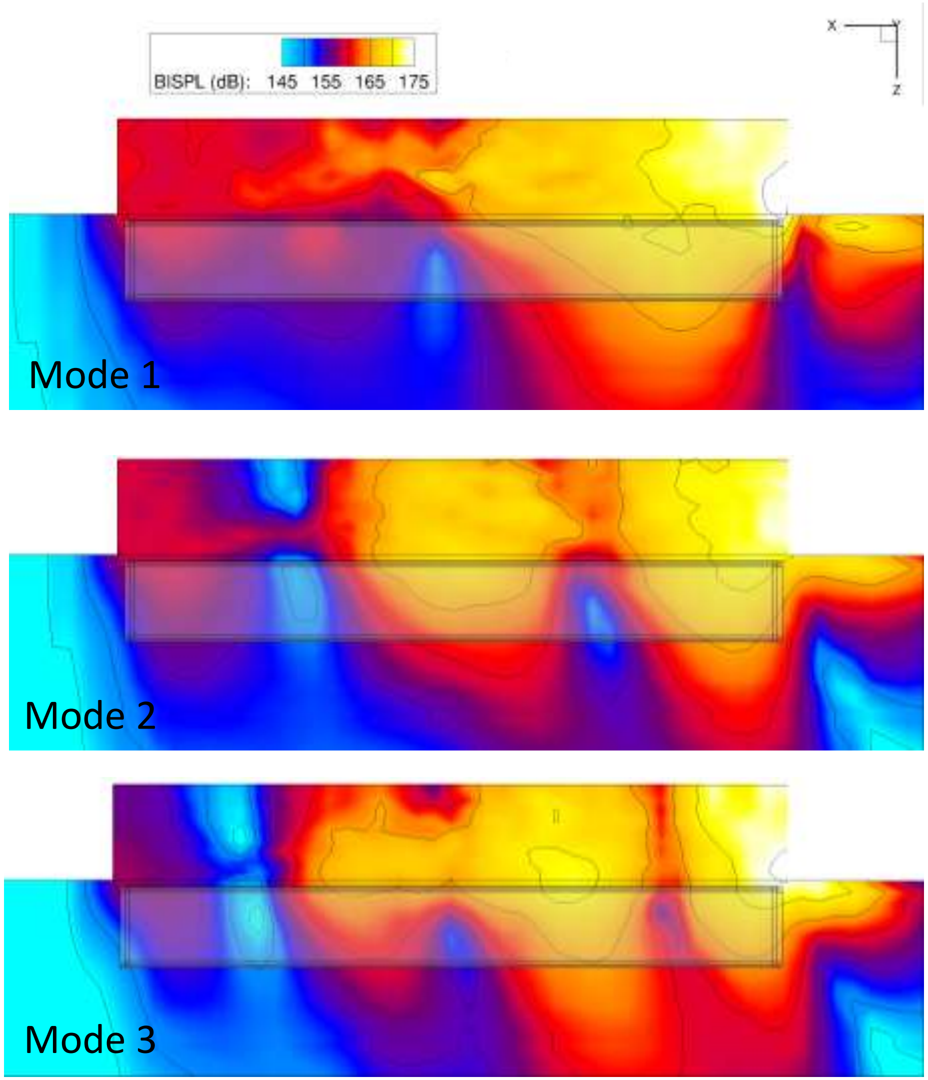

BISPL for modes 1 to 3 (Doors 110 degrees).

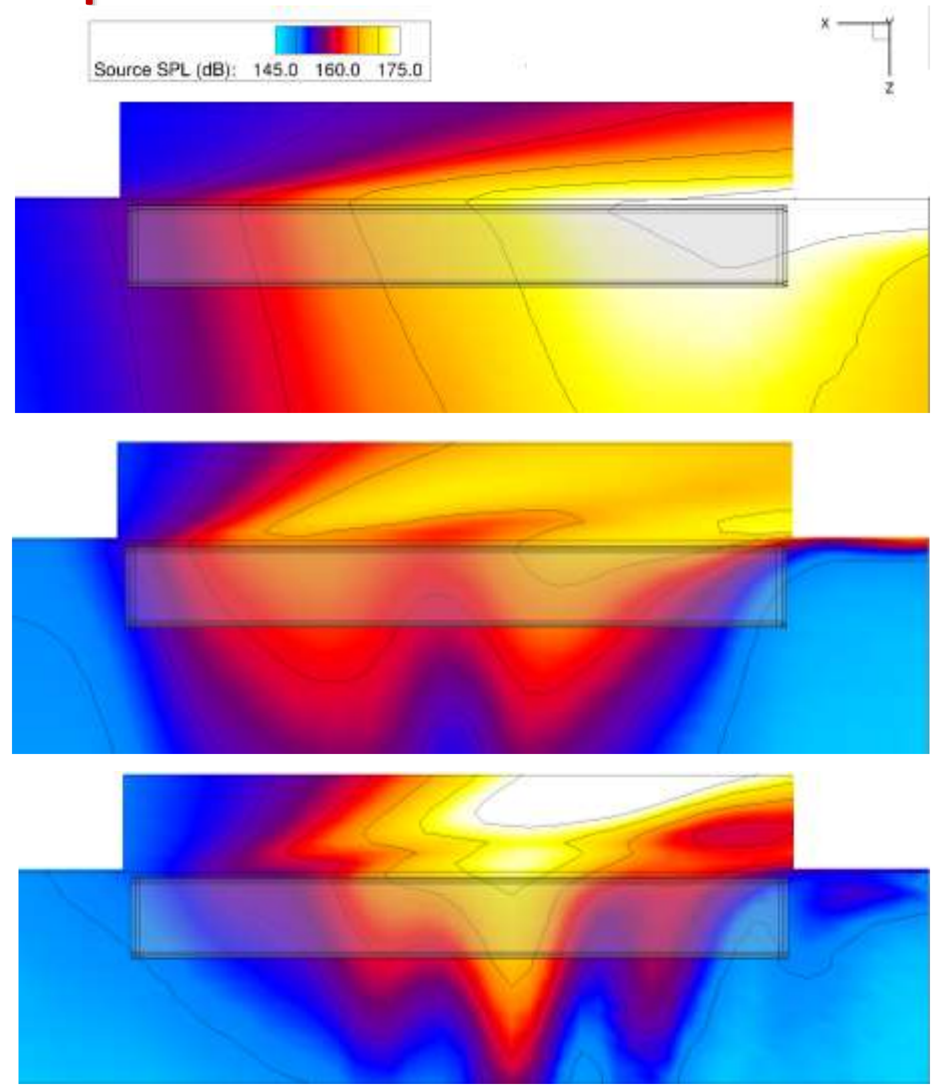

Beamforming for modes 1 to 3 (Doors 110 degrees).

Wavelet Transform

- A spectral decomposition of a signal shows what are the **main frequencies** but does not show **when they appear.**
- The Wavelet Transform shows the **distribution of the energy** in the **frequencies at every instance in time.**
- Give the **spatio-temporal fluctuations** of the pressure field.

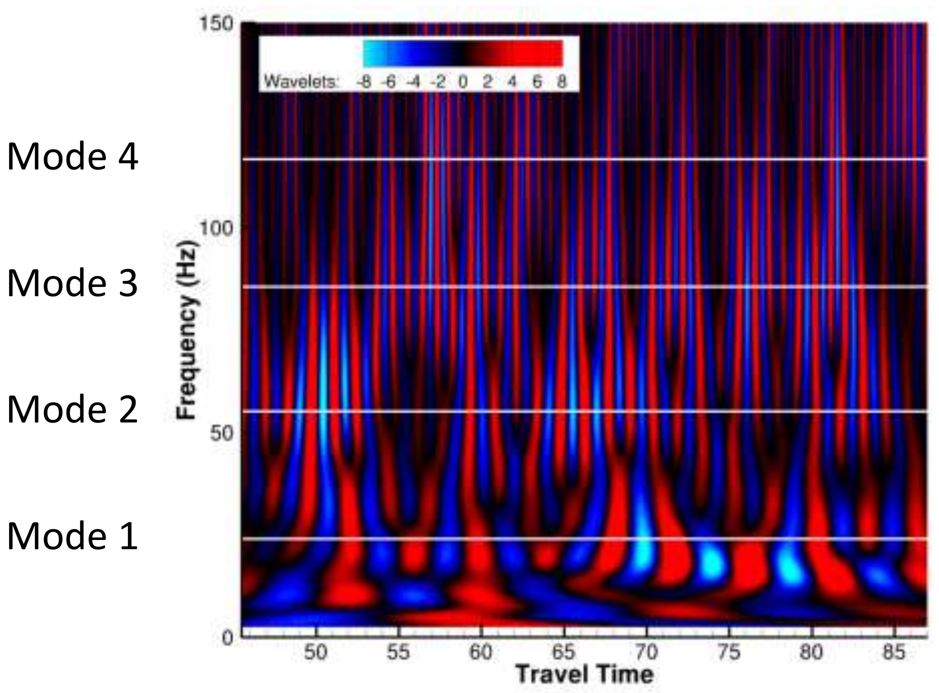

Scalogram for doors at 110 degrees at aft wall lip centre.

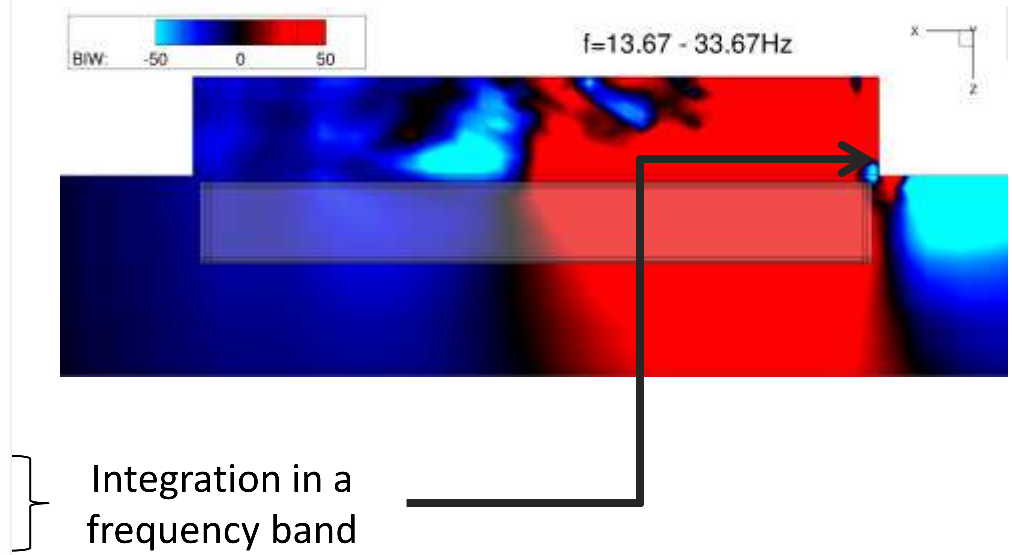

BIW at the cavity centreplan for mode 1 at an instance in time.

Cavity Flow Pressure Fluctuations

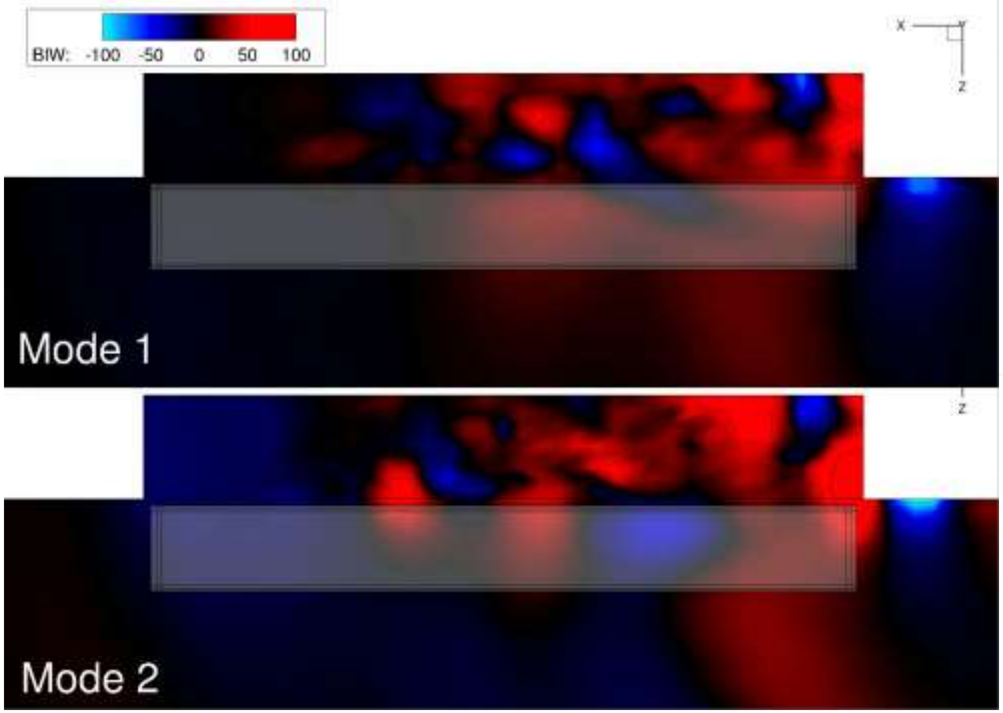

BIW at the cavity centreplan.

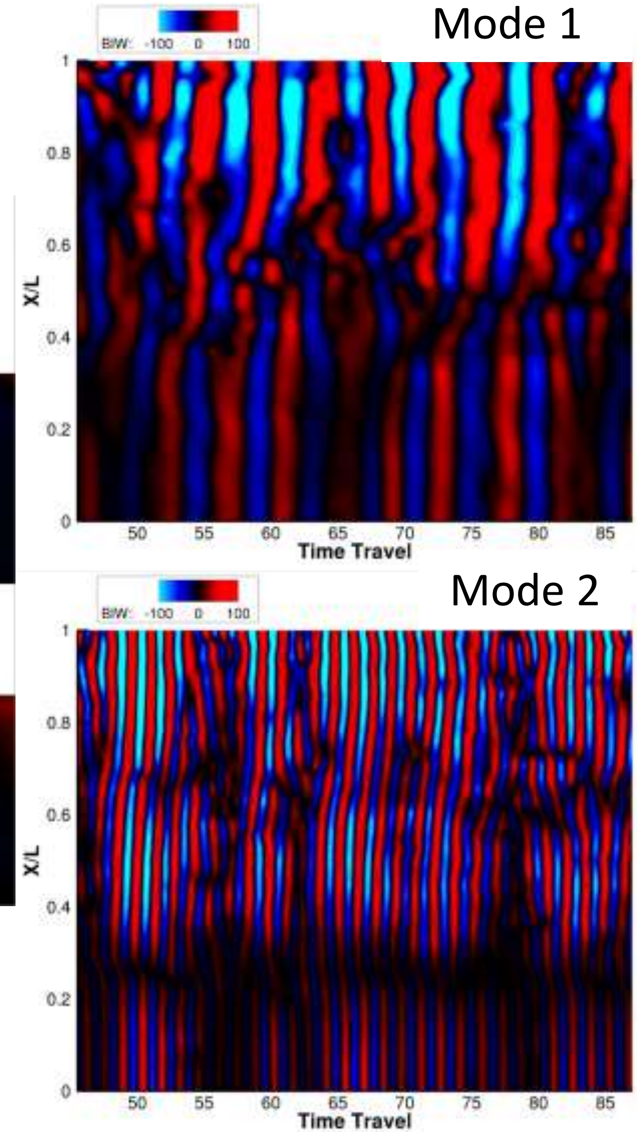

- **Nodes** and **antinodes**.
- **Phase opposition** between two antinodes.
- Cavity flow tones are produced by **standing waves**

BIW at the cavity ceiling for the store at carriage.

Cavity Flow Pressure Modulations

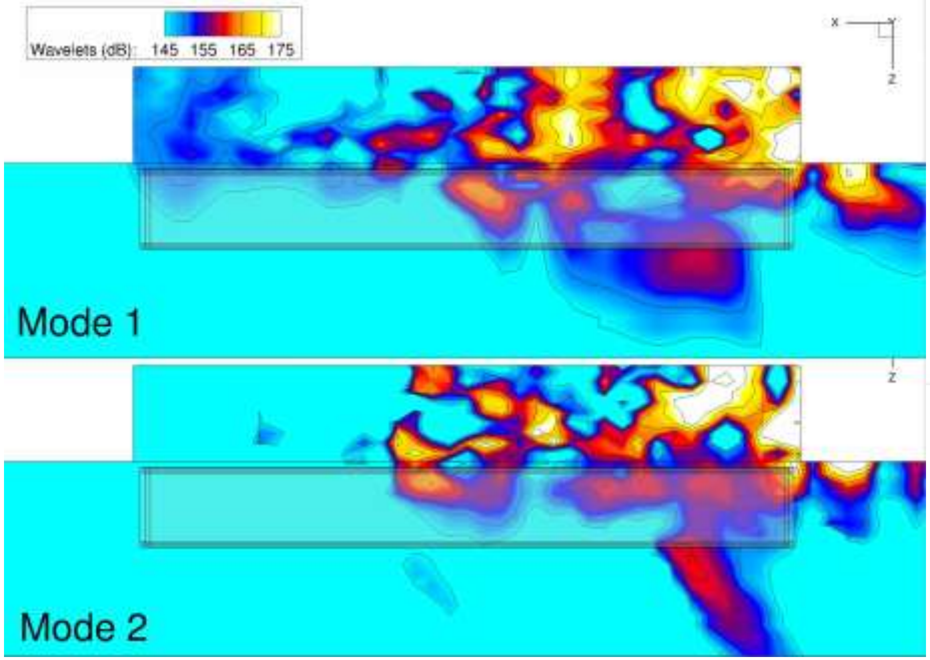

BIW envelop at the cavity centreline

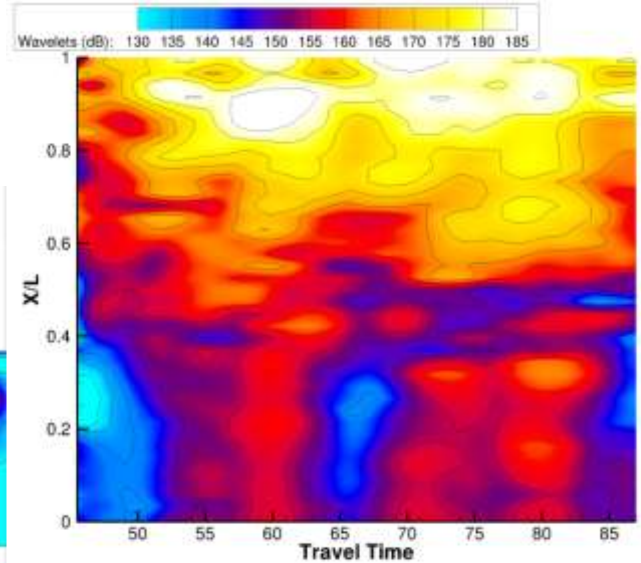

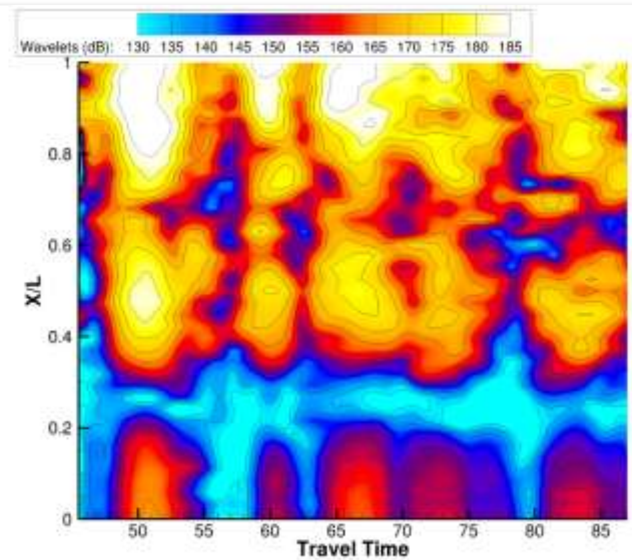

- BIW envelop show the peaks amplitude.
- The nodes and antinodes are more visible.
- The standing waves are **modulated in time**.

BIW envelop at the cavity ceiling for the doors at 110 degree.

M219 Pressure Fluctuations

- M219 Cavity experiments by Nightingale et al.

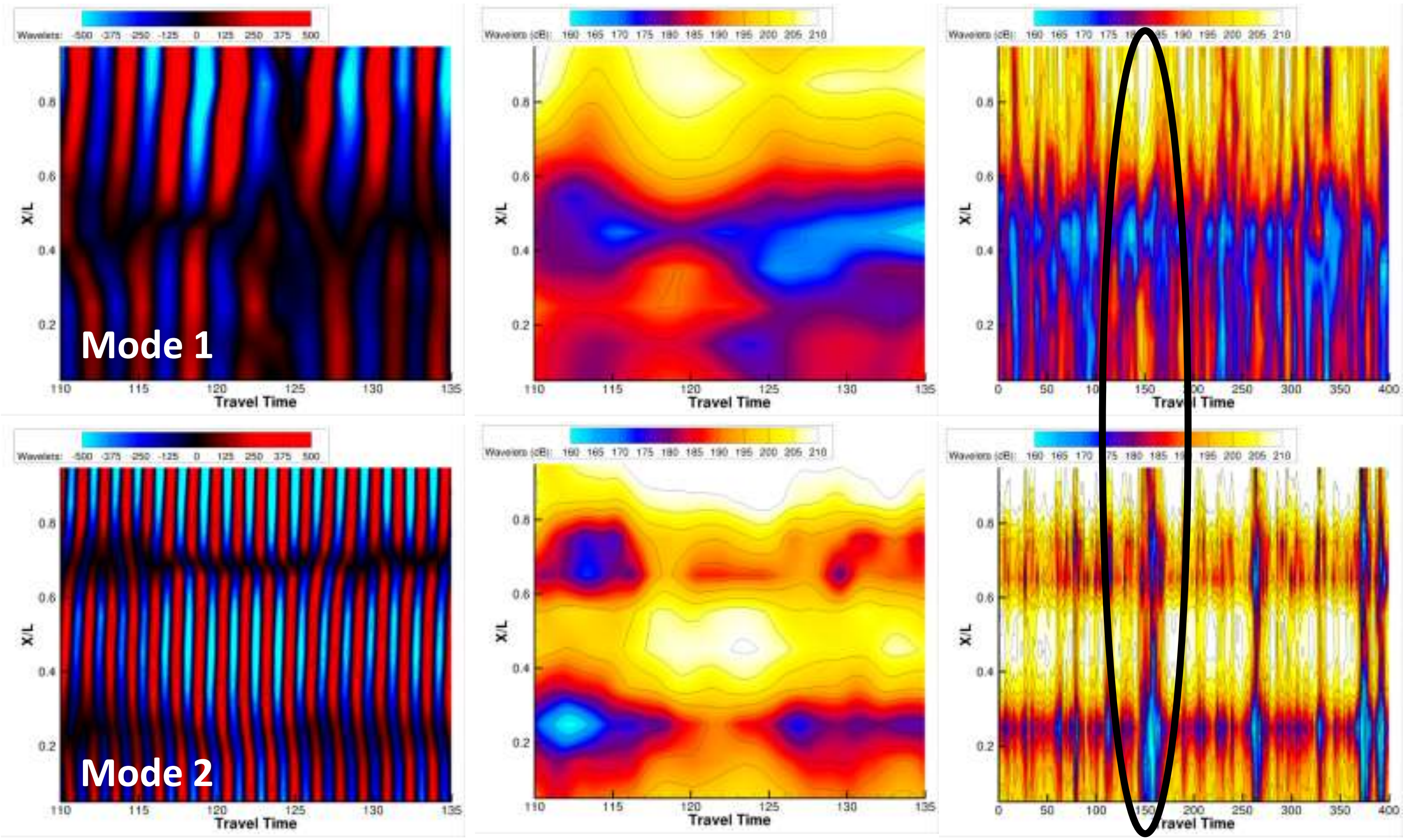

Standing waves. Standing wave modulation. Mode switching.

- Ideal cavity.
- M=0.85
- L/D=5
- Re_L: 6.5million
- 10 kulites along the ceiling
- 3 sec signal.

Cavity Flow Door Opening

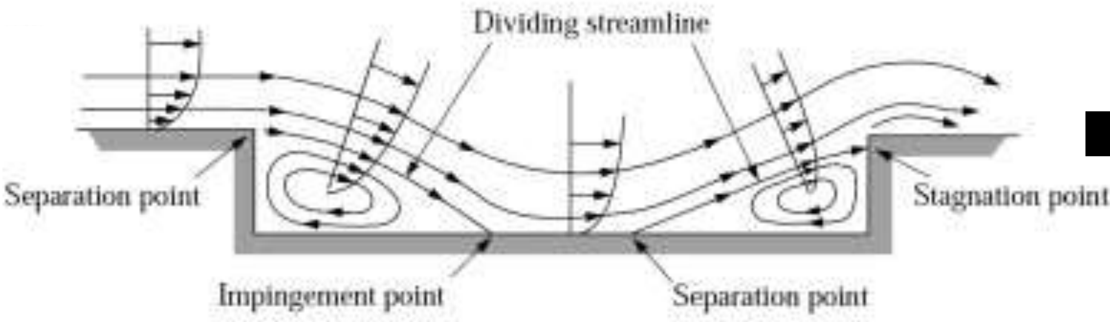

Closed cavity flow [1].

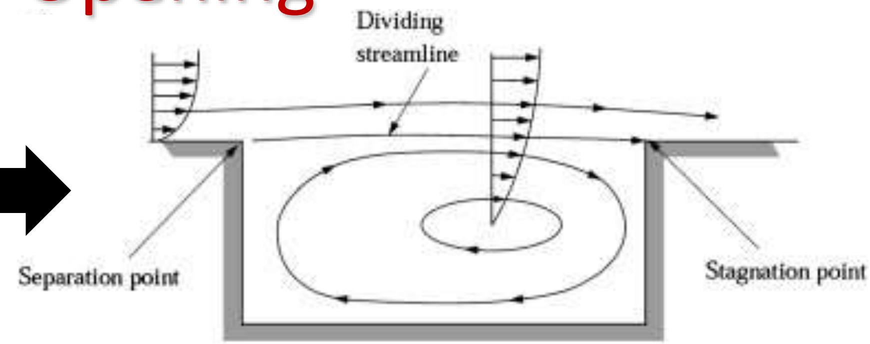

Open cavity flow [1].

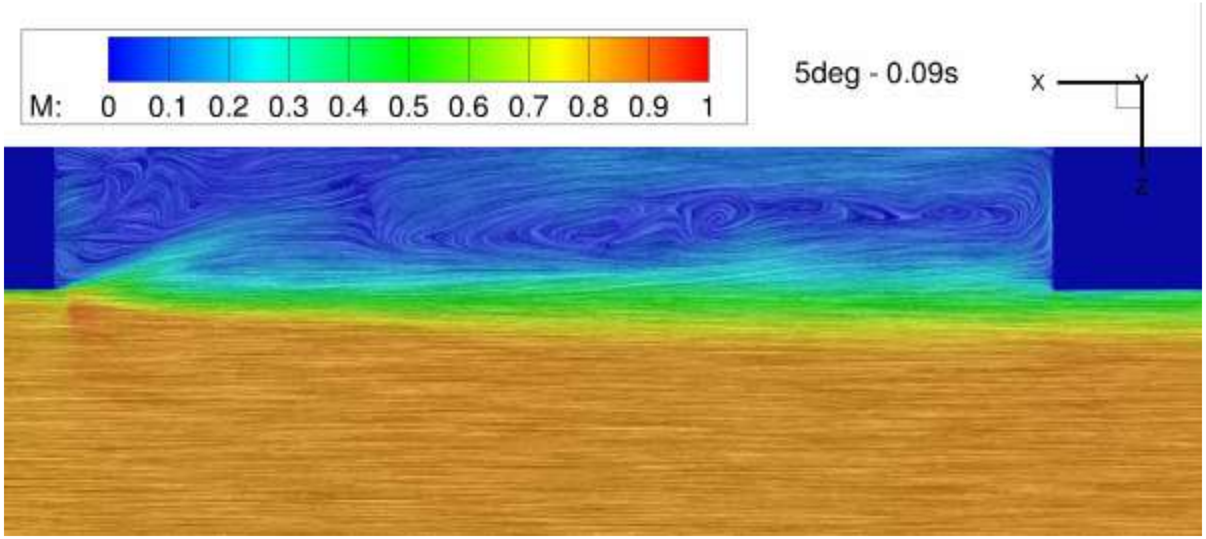

Cavity flow establishment during opening (220 deg/s). Mach Number and LICs at centreplan.

[1] Chappell, P. and Gilbey, R. W., "Drag of a rectangular planform cavity in a flat plate with a trubulent boundary layer for Mach numbers up to 3. Part II: Open and transitional flows." Tech. rep., February 2002.

1. Initialisation:
   - Closed cavity flow.
   - The flow impinges the cavity ceiling.
   - A vortex forms at the cavity front.
2. Transition:
   - The **front vortex grows**.
   - The **attachment point** reaches the **aft wall**.
3. Shear layer development:
   - Open cavity flow.

Cavity Flow Door Opening

- The wavelet is able to **track transitory state** of the opening:
  - The **travel of the jet** is visible during transition.
  - The different door velocities show different transition strength.

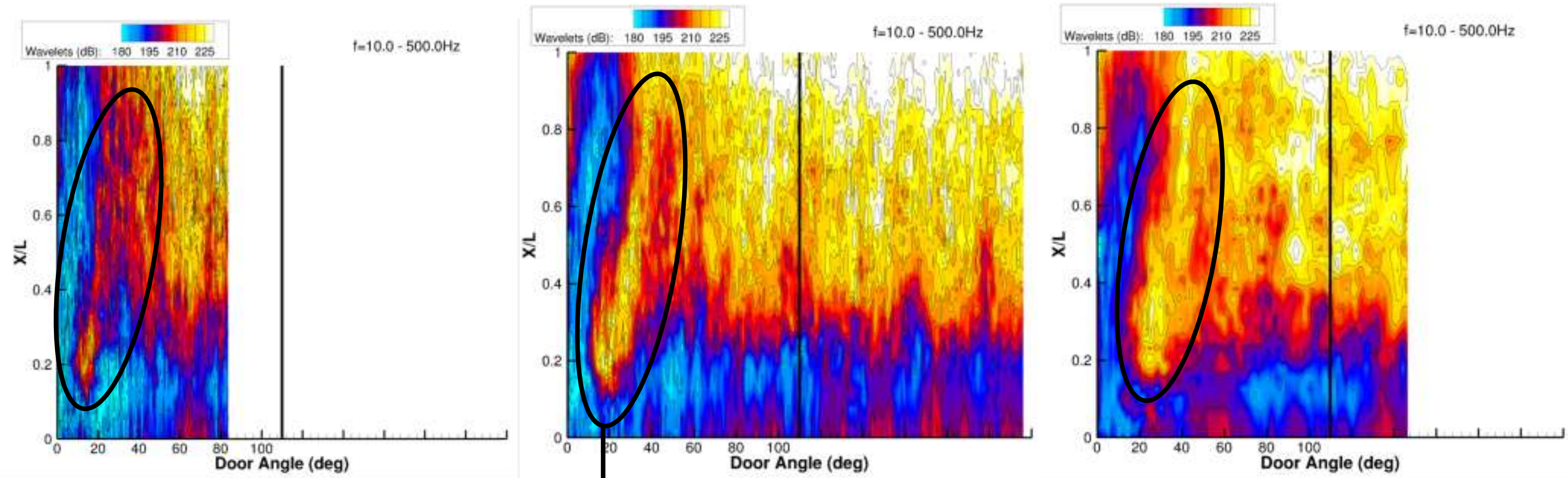

Slow - 110 deg/s

Medium - 220 deg/s

Fast - 440 deg/s

Jet path

Spatio-temporal fluctuations along the cavity ceiling of the cavity opening.

Cavity Flow Door Opening

- The mode 1 is **trigged by the transition**.
- The modes 2 and 3 noticeably increase from 70 degrees.
  - **Pacifying effect** of the doors for small angle.

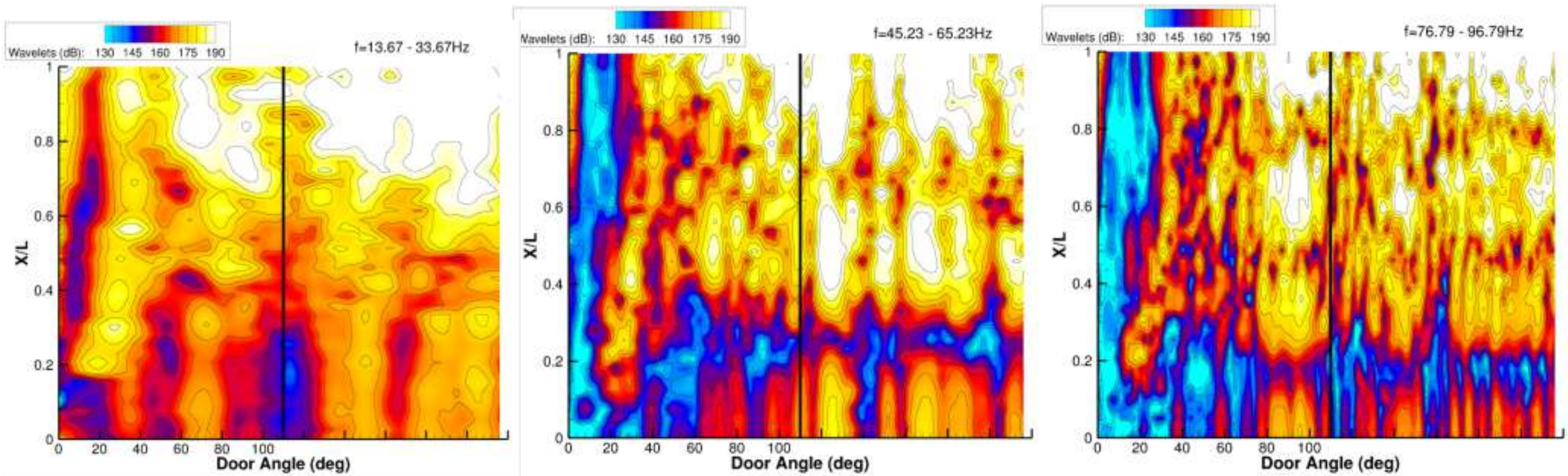

Mode 1 | Mode 2 | Mode 3

Spatio-temporal fluctuations along the cavity ceiling of the cavity opening (220 deg/s) for modes 1 to 3.

Noise Propagation

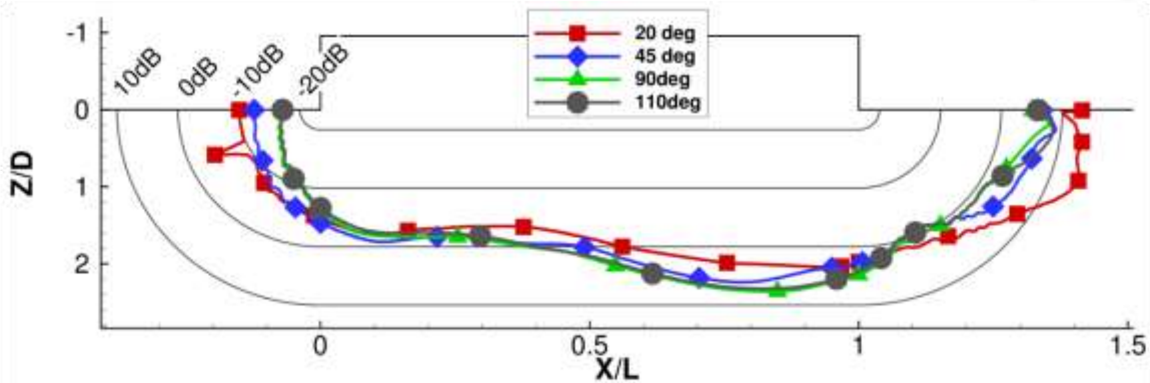

Noise directivity at 2 cavity depths from the shear layer.

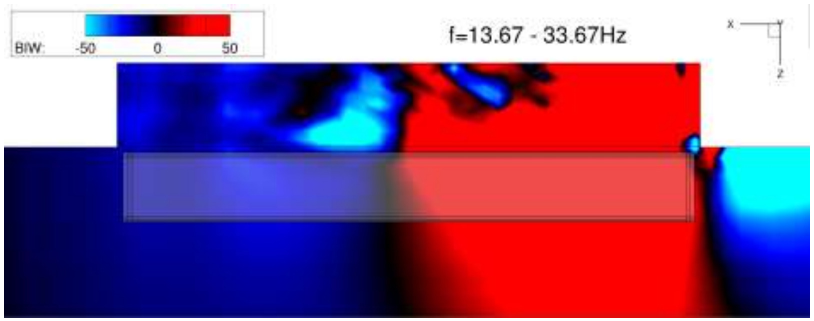

BIW for 14 – 34Hz

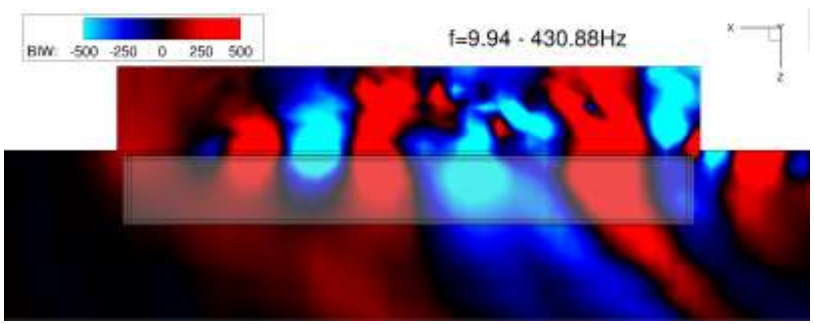

BIW for 10 – 430Hz

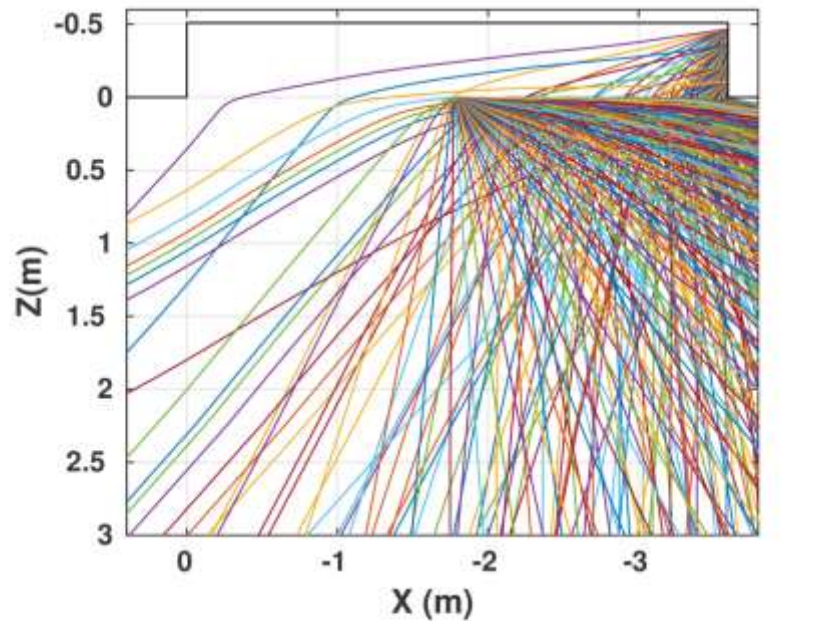

Simulation of the noise propagation with the full wave propagation model.

- The directivity is larger over the second half of the cavity.
  - The **flowfield transport the sound waves downstream**.
  - More noise is generated at aft wall.

Summary and Conclusion

- Beamforming:
  - The mean **flowfield has to be taken into account** to be accurate.
  - Able to **localise the main sources** of noise at the shear layer.
  - Captures the **mode shapes**.
  - Applicable to **wind tunnel** with **PIV measurements**.

- Wavelet transform:
  - Extracts the **spatio-temporal** fluctuations of the noise.
  - Exhibits a **standing wave** like behaviour for shallow cavity flow.
  - Tracks the noise fluctuations of **unsteady phases** of cavity flow.

- Noise propagation:
  - The flowfield has large influence on the noise propagation.
  - A large part of the noise radiate over the second half of the cavity.